

Dynamics of phase separation in two-dimensional tricritical systems

Paramdeep S. Sahni and J. D. Gunton

Physics Department, Temple University, Philadelphia, Pennsylvania 19122

Sheldon L. Katz and Roy H. Timpe

Physics Department, Lafayette College, Easton, Pennsylvania 18042

(Received 22 May 1981)

We present a Monte Carlo study of the tricritical spinodal decomposition of a two-dimensional model obeying Kawasaki dynamics which describes both an Ising metamagnet as well as a simple model of chemisorption. Quenches to three different points in the unstable domain are studied. In all cases the structure functions for both the nonconserved order parameter and conserved secondary order parameter exhibit dynamical instabilities as manifest by peaks which increase with increasing time. Each structure function satisfies a simple scaling behavior with respect to characteristic lengths whose time dependence can be approximated by simple power-law behavior in certain domains of time. In addition we find that the tricritical spinodal decomposition exhibits an unusual asymmetry with respect to the quench value of the conserved variable (the magnetization) as compared to the case of simple binary alloys. Namely, the peak in the magnetic structure factor (at fixed time) increases with increasing magnetization as one moves from one side of the unstable region toward the other side of the coexistence curve. Eventually, however, as one continues to increase the magnetization this peak value ceases to increase, but rather decreases dramatically in a very narrow transition region. This sharp transition would seem to be a fundamental dynamical distinction between tricritical and critical instabilities.

I. INTRODUCTION

A system which is suddenly cooled from a high-temperature, spatially homogeneous, one-phase state to a thermodynamically unstable state below its coexistence curve will begin to phase separate by a process known as spinodal decomposition. Its final equilibrium state will consist of macroscopic domains of coexisting phases. During this process of phase separation the initial homogeneous state dynamically evolves through highly inhomogeneous states which are far from equilibrium. If the time necessary to reach equilibrium is sufficiently long, this interesting, nonlinear dynamical process can be experimentally investigated. The class of systems which has been most commonly studied consists of binary alloys^{1,2} such as Al-Zn. Extensive Monte Carlo (MC) studies³⁻⁷ of kinetic Ising models for such alloys also exist. A wide range of other systems have also been investigated, including glasses,⁸ polymers,⁹⁻¹² and binary fluids.¹³⁻¹⁷ Quite recently studies of spinodal decomposition have also been initiated for systems quenched below tricritical points. In particular, Hohenberg and Nelson¹⁸ have presented a Cahn-Hilliard-like linear stability analysis for the initial stages of tricritical phase separation in ³He-⁴He mixtures. This binary phase decomposition has subsequently been studied experimentally by Hoffer,

Campbell, and Bartlett¹⁹ and Benda, Alpern, and Leiderer.²⁰ In addition, Sahni and Gunton²¹ have presented a Monte Carlo study of spinodal decomposition for a model of a two-dimensional Ising metamagnet satisfying Kawasaki dynamics in which both nearest and next-nearest neighbor pairs of spins are allowed to exchange. Since this metamagnet is also known to be a lattice gas model of atoms adsorbed on substrates, this Monte Carlo work can equally well be thought of as a study of the phase separation of ordered regions of $c(2 \times 2)$ islands in a sea of vacancies, in which adatoms are allowed to diffuse to empty nearest or next-nearest neighbor sites. This Monte Carlo work confirmed the prediction of Hohenberg and Nelson that both the nonconserved order parameter (the sublattice magnetization M_s for the metamagnet) as well as the conserved secondary order parameter (the magnetization M) exhibit dynamic instabilities. The Monte Carlo analysis, in particular, showed that the corresponding circularly averaged structure factors for M_s and M exhibit peaks as a function of wave number which increase with increasing time. In addition, these two structure functions were shown to exhibit a notable scaling behavior for sufficiently late times, quite similar to that found in Monte Carlo studies of binary alloys^{7,22} and order-disorder transitions,^{23,24} as well as in experimental studies of spinodal decomposition in

binary fluids¹⁵ and alloys.^{2,25} Specifically, the scaling of a given structure function $S(k,t)$ means that $S(k,t) = K^{-d}F(k/K(t))$ where $K^{-1}(t)$ is some characteristic time dependent length, k is the wave number, and d is the dimensionality. This homogeneous property of the structure function is perhaps the most significant new feature to have been observed in recent studies of spinodal decomposition. No detailed, first principle theory for such scaling yet exists, although predictions of scaling behavior have been obtained in a variety of recent theoretical investigations.^{26,27}

In this paper we extend our Monte Carlo study of the tricritical spinodal decomposition and growth mechanisms for the same system as studied in Ref. 21. Namely, we consider an Ising model of a two-dimensional metamagnet whose spins are at the vertices of a square lattice. In addition to a magnetic field energy, the Hamiltonian contains nearest-neighbor antiferromagnetic and competing next-nearest-neighbor ferromagnetic interactions. By a standard transformation discussed in Sec. II, this Hamiltonian can also be considered to be a lattice gas model of adatoms on a substrate. In particular, this Hamiltonian has been used as a simple model of the chemisorption systems (Ref. 28) H/W(001) and O/Cu(001).²⁹ However, recent theoretical work³⁰ indicates that the effects of a substrate distortion must also be taken into account to obtain a correct description of H/W(001). Thus our dynamical study can only be taken as a simple approximation for such chemisorption systems. A model study of the dynamics of phase separation in O/W(110) will be reported later.³¹ In this paper our discussion will be given in terms of the metamagnet. In this case the two phase coexistence consists of a paramagnet phase with a nonzero magnetization (resulting from the applied field) with a vanishing sublattice magnetization in equilibrium with an ordered antiferromagnetic phase, as can be seen from Fig. 1(a). After a quench from a high-temperature "disordered" paramagnetic phase, the metamagnet then spinodally decomposes into antiferromagnetic droplets (islands) in a paramagnetic sea. Two types of antiferromagnetic droplets can be defined, differing from each other only by a simple translation of one lattice constant. If one chooses to interpret the Hamiltonian as a model of adatoms on a substrate, the two phase coexistence consists of an ordered $c(2 \times 2)$ structure^{28,29} adatoms in equilibrium with a fluidlike phase dominated by vacancies as shown in Fig. 1(b). After a quench from a high-temperature "disordered" fluid phase, this chemisorption system would then phase separate into ordered islands of $c(2 \times 2)$ structure in a sea of vacancies. In both the metamagnet and the chemisorption model, we consider the conventional Kawasaki dynamics in which only nearest-neighbor exchange is allowed. In the metamagnet this corre-

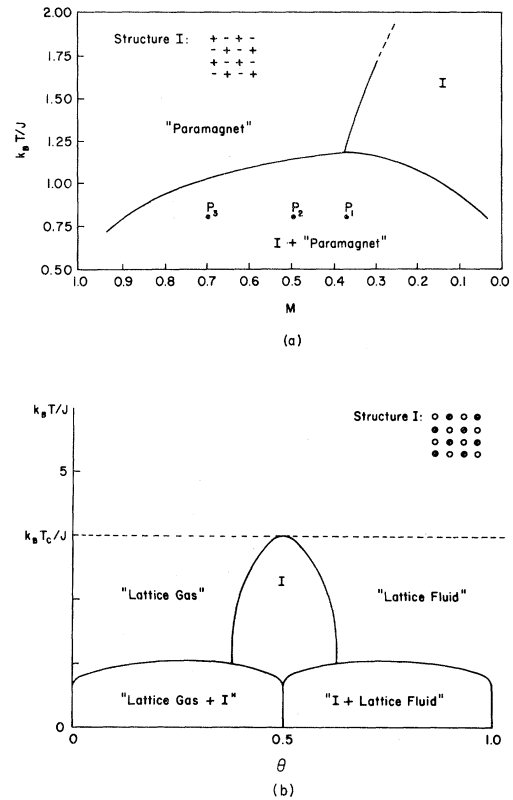


FIG. 1. Schematic phase diagrams for (a) metamagnet (b) lattice-gas model.

sponds to exchange of nearest-neighbor spins and in the chemisorption system to an adatom hopping to a vacant nearest-neighbor site. We will call this nearest-neighbor exchange system model I. This dynamics differs from the original Monte Carlo study²¹ for a system with the same Hamiltonian in that in the previous work next-nearest-neighbor exchange was also allowed. We will call this second system model II. The differences in the phase separation process for these two different models are discussed in Sec. IV.

As shown in Fig. 1, we have studied quenches to three particular unstable states P_1 , P_2 , and P_3 . These states correspond to a low-temperature value of $T \approx 0.66 T_i$ and a magnetization per spin of $M = 0.37$, 0.5 , and 0.7 , respectively. In the original work²¹ we only considered the quench to P_2 . It should also be noted that the exact phase diagram for this Hamiltonian is not known. The most accurate determination of the tricritical point appears to be a recent Monte Carlo real-space renormalization-group analysis³² which suggests that the tricritical point is given by $T_t \approx 1.21J/k$, $M_t \approx 0.37$, where J is the nearest-neighbor exchange constant. This is somewhat different from an earlier standard Monte Carlo³³ estimate of $T_t \approx 1.30J/k$, $M_t \approx 0.45$. The estimates

for the coexistence curve given in this Monte Carlo study are still thought to be accurate, however. It should also be noted that we have no first principle knowledge that P_1 , P_2 , and P_3 are all unstable states, rather than metastable states. Indeed studies of simple binary alloys indicate that the distinction between unstable and metastable states is in any event not sharp.

The main results of our present investigation are the following. We find the same type of dynamical instabilities in the nonconserved order parameter and conserved secondary order parameter as in the case of model II in which next-nearest-neighbor exchanges are also allowed. Namely, for the three points P_1 , P_2 , and P_3 the order-parameter structure function $S_{M_s M_s}(k, t)$ exhibits a peak in the vicinity of $k = 0$ which increase with increasing time. Similarly the structure function $S_{MM}(k, t)$ for the conserved variable exhibits a peak at a nonzero value of k , $k_m(t)$, with $k_m(t)$ decreasing and $S_{MM}(k_m(t), t)$ increasing with increasing time. Both structure functions exhibit a simple scaling form for P_1 , P_2 , and P_3 for a large region of time which excludes an initial "transient" behavior. However, our results for scaling at P_1 are less convincing than for P_2 and P_3 due in part to a kind of "metastability" which develops there. Our results for the nonconserved variable are particularly sensitive to this metastability for small values of k , as we discuss in the text. The time-dependent scaling length for $S_{MM}(k, t)$ is taken to be its first moment. The scaling length for $S_{M_s M_s}(k, t)$, which is an even function of k , is taken to be the square root of its second moment. The respective scaling functions F and G for $S_{MM}(k, t)$ and $S_{M_s M_s}(k, t)$ also depend on some extent on the variable M ; i.e., they are different for the different P 's studied. This dependence of a scaling function on a conserved variable has also been observed in extensive Monte Carlo studies⁷ of a three-dimensional Ising model of a binary alloy. We should emphasize the fact that we cannot claim to *prove* that the structure functions scale. Rather we can simply say that to a first approximation our data are consistent with a scaling form. This qualification is presumably also true of previous studies of binary alloys and binary fluids. It should also be noted that there is some evidence of a weak deviation from scaling in our work, in that the ratio of various moments seem to exhibit a rather small dependence on time. If scaling were strictly correct, such ratios should be time independent.

Another interesting result is the existence of an asymmetry in this tricritical phase separation which is absent for binary alloys. Namely, the structure function $S_{MM}(k, t)$ exhibits a peak which at a fixed time increases with increasing M in the domain of instability which we have studied, rather than exhibiting a

symmetry about a critical value of M which represent the maximally unstable point. The latter is the situation for a symmetric binary alloy where M represents the concentration of one of the species of atoms. This tricritical asymmetry is in agreement with what one might expect from the mean-field linear stability analysis of Hohenberg and Nelson.¹⁸ In their analysis the effective susceptibility which provides the driving force for the initial stages of phase separation of the conserved variable becomes more negative as one increases the magnetization in the unstable region, thus leading to an asymmetry in the structure function. This same feature is found in a more extensive Langer, Bar-on, and Miller³⁴-type analysis of Dee, Gunton, and Kawasaki³⁵ which treats approximately the nonlinearity of the problem. What seems even more interesting about this asymmetry is that as we increase M beyond a certain value $M \approx 0.88$, we find that the maximum value of S_{MM} (at fixed time) decreases rather dramatically. It is difficult to give a precise interpretation of this sharp transition. If one uses the mean field, linearized dynamical theory as a guide, then this transition would correspond to passing from an unstable to a metastable state at a value of the magnetization which would be a spinodal point. That is, the effective susceptibility would change from being negative to positive as one passes through this spinodal value, with a consequent decrease in the maximum in the structure function. However, it is by now reasonably well established that a sharp spinodal curve which would possibly distinguish between instability and metastability does not exist for systems with short-range forces, so that the above is probably not a strictly correct interpretation. Nevertheless, it would seem likely that any successful nonlinear theory of this transition will involve this asymmetric effective susceptibility, so that the sharp transition would seem to be directly related to this quantity. Whether this transition we see is a crossover from instability to metastability, in the classical sense, is much less clear. In any event, this behavior seems to be a major distinction between the nonlinear instabilities exhibited by tricritical and critical systems and poses an interesting challenge for theoretical interpretation.

We should also note that our results for $S_{MM}(k, t)$, apart from this asymmetry, are quite similar to the corresponding structure function for the binary alloy. Thus in this sense certain aspects of tricritical phase separation are similar to critical phase separation. However, the exponents which characterizes the first moment of $S_{MM}(k, t)$ in our scaling region differs from the Lifshitz-Slyozov³⁶ exponent reported in the Monte Carlo studies⁷ of the binary alloys. This is possibly due to the fact that our system evolves more slowly than the Ising model of the binary alloy so that our study does not include the late stage region in which the Lifshitz-Slyozov law is valid.³⁷ It should

also be noted that it is difficult to make a definitive determination of the exponents in these studies so that the differences between our exponent and that obtained in the binary alloy work might not be that significant. Finally we stress that our results for the nonconserved order-parameter structure function, $S_{M_s M_s}(k, t)$, are less reliable than for $S_{MM}(k, t)$, in that they seem extremely sensitive to finite-size effects. Namely, our estimates for the approximate power-law dependence of the moments of this function are significantly different depending on whether or not we include the $k=0$ value of $S_{M_s M_s}(k, t)$ in our analysis. For a bulk system the results for the structure function should not depend on the nature of the boundary condition. However, for a finite system with free boundaries, the smallest wave number should be $k=2\pi/L$ where L is the edge size, rather than the $k=0$ value appropriate for periodic boundary conditions. Therefore as a check on finite-size effects we have analyzed our moments and scaling behavior for both models I and II with and without the $k=0$ data. We have found that the results which are most consistent with scaling are those which exclude the $k=0$ data, as we discuss in the text. In addition, models I and II show no significant dynamical differences if we exclude the $k=0$ data, but differ considerably in estimates of the time dependence of the moment of $S_{M_s M_s}(k, t)$ if we include the $k=0$ data.

In Secs. II and III we present our Monte Carlo results for the nearest-neighbor exchange model. In addition to discussing the structure functions and their scaling forms, we also present an analysis of various moments of these functions, to see to what extent the data is consistent with the scaling concept. We stress there that a more sensitive criterion for scaling is to consider whether the ratio of appropriate moments is time independent, rather than to simply seek scaling of the data. Power-law approximations are also given for the time dependence of some of these moments, although it is unclear as to the ultimate significance of such fits. It should be noted that just as in the Monte Carlo studies of the binary alloy,⁷ almost any assumed form with some adjustable parameters can be made to fit our data. However, theories such as Lifshitz-Slyozov do predict power-law behavior in certain domains of time, so it seems reasonable to attempt a power-law analysis. In Sec. II we also show some typical configurations characteristic of various stages of the phase separation process. The growth of antiferromagnetic clusters in the paramagnetic background is clearly seen. In Sec. IV we briefly review the results of the previous Monte Carlo study which includes next-nearest-neighbor exchange (model II). Some new results for this model are also presented. We also compare the dynamical evolution for these two models. Finally, in Sec. V we present some brief concluding remarks.

II. MONTE CARLO RESULTS FOR MODEL I

A. Model I

The Hamiltonian for the two-dimensional metamagnet is taken to be

$$H = J \sum_{\text{NN}} \sigma(\vec{r}) \sigma(\vec{r}') - \alpha J \sum_{\text{NNN}} \sigma(\vec{r}) \sigma(\vec{r}'') - H \sum_{\vec{r}} \sigma(\vec{r}) \quad , \quad (2.1)$$

where the vector $\vec{r} = m\hat{a} + n\hat{b}$ with \hat{a} and \hat{b} unit vectors and m and n take integral values between 1 to \sqrt{N} . The N spins $\sigma(\vec{r}) = \pm 1$ are located at the vertices of a square lattice. There is a competition between the nearest-neighbor NN antiferromagnetic interactions and the next-nearest-neighbor NNN ferromagnetic interactions which, together with the magnetic field energy, leads to a phase diagram which is given approximately in Fig. 1(a). For the case $\alpha=0.5$ studied in this paper, recent Monte Carlo real-space renormalization-group work³² suggests that the tricritical point is given by $T_t \approx 1.21J/k_B$ and $H_t \approx 3.283$ with the value of M_t being less certain but approximately given by $M_t \approx 0.37$. The dynamics of this model I is taken to be Kawasaki spin exchange in which nearest-neighbor spins $\sigma(\vec{r})$, $\sigma(\vec{r}')$ are allowed to exchange with a transition probability

$$W_{\vec{r}, \vec{r}'} = \alpha_s \frac{\exp(-\Delta H_{\vec{r}, \vec{r}'}/k_B T)}{1 + \exp(-\Delta H_{\vec{r}, \vec{r}'}/k_B T)} \quad , \quad (2.2)$$

where $\Delta H_{\vec{r}, \vec{r}'}$ is the change in energy which results from the interchange and α_s^{-1} set the unit of time. The system satisfies a master equation for the time-dependent probability distribution functional describing the probability of a given configuration of spins, with $W_{\vec{r}, \vec{r}'}$ providing the mechanism for dynamical evolution. We simulate the dynamical properties of this system by standard Monte Carlo procedures, using a 60×60 lattice with periodic boundary conditions. The various quantities which we monitor include the energy per site and the sublattice magnetization

$$M_s = N^{-1} \sum_{\vec{r}} (-1)^{m+n} \sigma(\vec{r}) \quad . \quad (2.3)$$

We also calculate the structure factors for the local sublattice magnetization and magnetization which in our Monte Carlo calculation are given by

$$S_{M_s M_s}(\vec{k}, t) = N^{-1} \left| \sum_{\vec{r}} e^{i\vec{k} \cdot \vec{r}} (-1)^{m+n} \sigma(\vec{r}) \right|^2 \quad (2.4)$$

and

$$S_{MM}(\vec{k}, t) = N^{-1} \left| \sum_{\vec{r}} e^{i\vec{k} \cdot \vec{r}} [\sigma(\vec{r}) - \langle \sigma \rangle] \right|^2 \quad . \quad (2.5)$$

We follow the usual procedure used in Monte Carlo studies of this kind of defining circularly averaged structure functions

$$S(k, t) = \frac{\sum_{\{\bar{k}\}} S(\bar{k}, t)}{\sum_{\{\bar{k}\}} 1}, \quad (2.6)$$

where the sum over $\{\bar{k}\}$ is over all values of \bar{k} such that

$$\frac{2\pi}{\sqrt{N}}(j - \frac{1}{2}) < |\bar{k}| \leq \frac{2\pi}{\sqrt{N}}(j + \frac{1}{2}), \quad (2.7)$$

where $j = 0, 1, 2 \dots 10$. This allows us to reduce our data to a more practical level. Note that it is easy to obtain certain simple values for these structure functions, such as

$$S_{M_s M_s}(k=0, t) = NM_s^2(t) \quad (2.8)$$

and

$$S_{MM}(k=0, t) = 0. \quad (2.9)$$

In addition there is the sum rule

$$N^{-1} \sum_{\{\bar{k}\}} S(\bar{k}, t) = 1 - M^2, \quad (2.10)$$

which in our MC calculation is only approximately satisfied, as we discuss later, due to our only including values of j out to 10 in the actual calculations. The dynamical processes which we consider in this paper correspond to three particular quenches shown in Fig. 1(a). In each case the system is initially prepared in a thermal equilibrium at an essentially infinite temperature ($T = 4000J/k_B$) and then quenched to a state P_1 , P_2 , or P_3 below the coexistence curve. Each quench is performed at a constant magnetization, i.e., at $M = 0.37, 0.5$, and 0.7 , respectively. After a quench to one of the states P_i , the system is then monitored, starting from this $t=0$ unstable state. In general averages of the various quantities of interest are performed over six different runs. In addition, to check our statistics, three additional runs were performed at P_1 and P_3 . The resultant structure functions calculated from the averages over these nine runs were almost identical to the structure functions calculated from the averages over six runs. Finally, to check for finite-size effects we performed one run for a 100×100 lattice at $M = 0.37$. Although the results of this run were not identical with those obtained from the average over nine runs, the deviations were comparable to those obtained from run to run for the 60×60 lattice. Thus we think the results presented below are a reasonable representation of the dynamical evolution of this system. However, it is of course, always desirable to use larger lattices and average over a large number of runs to minimize the error involved in these computer simulations, although in practice time and expense impose limitations.

Before turning to a discussion of the results we

first summarize how the above Hamiltonian can be considered as a lattice gas model of a chemisorbed system. If one introduces the transformation

$$c(\bar{r}) = [1 - \sigma(\bar{r})]/2, \quad (2.11)$$

where $c(\bar{r}) = 0$ or 1 , then (2.1) transforms to

$$H = \phi_{NN} \sum_{NN} c(\bar{r})c(\bar{r}') - \alpha\phi_{NN} \sum_{NNN} c(\bar{r})c(\bar{r}'') + \epsilon \sum_{\bar{r}} c(\bar{r}) + H_0, \quad (2.12)$$

where

$$\phi_{NN} = 4J \quad (2.13)$$

and

$$\epsilon = 2H - 4J(1 - \alpha), \quad (2.14)$$

with H_0 representing an unimportant background term. In this representation the Hamiltonian given in (2.13) represents a model of adsorbed monolayer on a surface, in which atoms are adsorbed at certain sites of a square lattice which represents the substrate. The local occupation number $c = 0, 1$ depending on whether the site \bar{r} is vacant or occupied by an adatom. The coverage θ of the surface is then given by $\theta = \langle c(\bar{r}) \rangle$. The interaction between adatoms is given by the nearest-neighbor and next-neighbor interaction constants ϕ_{NN} and $-\alpha\phi_{NN}$, respectively, with the binding force between the adatom and the substrate lattice being ϵ . The analog of the sublattice magnetization is the order parameter ψ which describes the $c(2 \times 2)$ phase in the ordered state. It could be defined as $\psi = N^{-1} \sum_{\bar{r}} (-1)^{m+n} [2c(\bar{r}) - 1]$. The role of the magnetization M in the metamagnet is played by the coverage θ which is related to M by $\theta = (1 - M)/2$. The corresponding structure functions could be taken as $\langle \psi(\bar{r})\psi(\bar{r} + \bar{r}') \rangle$ and $\langle \delta\theta(\bar{r})\delta\theta(\bar{r} + \bar{r}') \rangle$. These are trivially related to the structure factors for the metamagnet, so that one can immediately interpret the results we present for the metamagnet in language appropriate to the lattice-gas system. It should be noted, however, that in this paper we do not monitor the time evolution of the "Laue" spot often studied in chemisorption systems.

B. Results

We begin by discussing some of the qualitative behavior characteristic of the phase separation process. We first compare the development of clusters following quenches for the two cases $M = 0.37$ and $M = 0.7$. (The situation for $M = 0.5$ is intermediate between these two cases.) First we consider the quench to P_3 . In Fig. 2(a) we show a typical high temperature, disordered paramagnetic configuration in

which the sublattice magnetization is zero. Shortly after the quench to the unstable point P_3 small clusters of antiferromagnetic order begin to develop in the paramagnetic sea and gradually grow as time progresses, as can be seen in Figs. 2(b)–2(f). A cluster of an antiferromagnetic order is defined as a set of up and down spins arranged such that each spin in the set has at least one of its nearest neighbors of the opposite kind. It should be noted that for purposes of display every alternate spin in a given configuration of the real system has been flipped and the resulting ferromagnetic clusters of up (and down) spins have been represented by squares (\square) and asterisks (*), respectively. Thus there are two types of antiferromagnetic clusters shown. These clusters have a net positive and negative sublattice magnetization M_s , respectively, and differ from each other only by a simple translation of one lattice constant. The paramagnetic background which consists of predom-

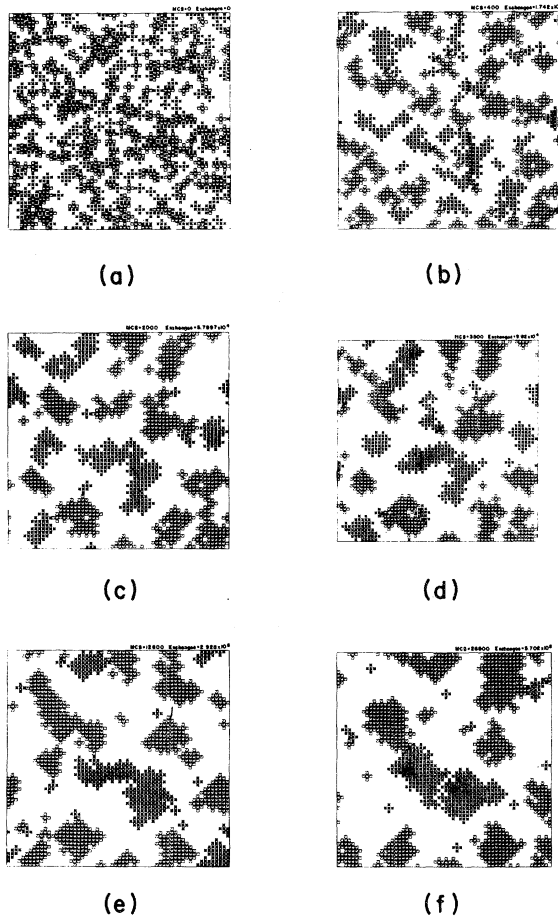


FIG. 2. Snapshots of the configurations for point P_3 for different times are displayed in (a)–(f). The clusters with asterisks and squares correspond to $+M_s$ and $-M_s$, respectively.

inantly up spins is simply shown as a white background in these figures. The situation is somewhat different for the quench to P_1 , where the paramagnetic background is substantially smaller than at P_3 due to the smaller magnetization. Again antiferromagnetic clusters form following quench and rapidly grow, as can be seen in Figs. 3(a)–3(d). However one encounters significantly more antiphase boundaries in which “plus” antiferromagnetic clusters share a boundary with “minus” antiferromagnetic clusters. The presence of these antiphase boundaries tends to slow down the growth process of such clusters. This is due to the fact that the boundary is always comprised of like spins and an exchange of like spins does not change the size of either of the two clusters sharing this antiphase boundary. Thus the motion of the antiphase boundary (the growth of clusters) only occurs as a result of a two-step spin exchange process which is statistically rather improbable. (This process would involve an exchange of nearest-neighbor unlike spins at the surface of one cluster, followed by an exchange of nearest-neighbor, unlike spins between the two clusters.)

Finally, we note that in all three quenches we encounter significant “metastability” in that the order parameter never reached its equilibrium value in any of the runs, even for times of the order of 42 000 Monte Carlo steps (MCS). This can be seen in Figs. 4(a) and 4(b), where some typical values for the time evolution of M_s are shown. In many cases the order parameter hovers around a value close to zero. As a

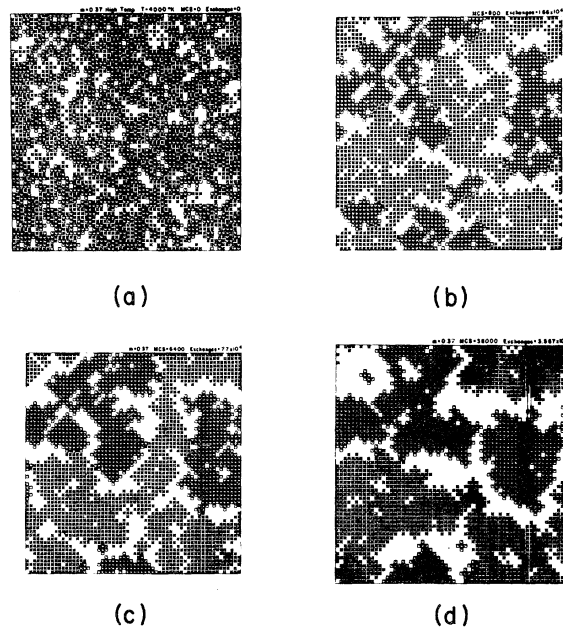


FIG. 3. Snapshots of the configurations for point P_1 for different times are displayed in (a)–(d).

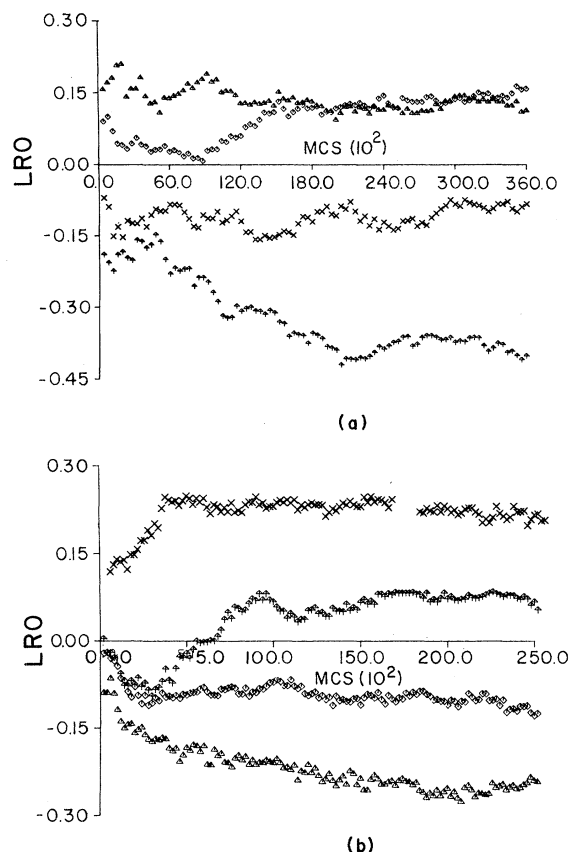


FIG. 4. Four sample runs of the order parameter M_s vs time for points (a) P_1 and (b) P_3 .

result of this and the relation (2.8) our values of the order-parameter structure function at $k=0$ are very sensitive to these metastable states. It has also been our observation that the values of $S_{M_s M_s}(k, t)$ at $j=1$ seem to weakly reflect this metastability, although we have no convincing argument as to why this should be so.

We now consider our results for the structure functions, beginning first with $S_{M_s m_s}(k, t)$. One qualitative feature of this quantity is that the peak develops at the origin and gradually grows, as can be seen in Figs. 5(a)–5(c). The best evidence for this can be seen in Figs. 5(b) and 5(c) for P_2 and P_3 . At P_1 our results are more sensitive to the problems of metastability mentioned above. A more precise characterization of the structure function at P_1 , P_2 , and P_3 can be given in terms of its moments, which we postpone until the next section when we discuss the evidence for the scaling of this structure function in the unstable domain.

A more interesting structure function which also seems less affected by the problems of “metastability” is $S_{MM}(k, t)$, which describes the fluctuations of the local magnetization. Since M is a conserved vari-

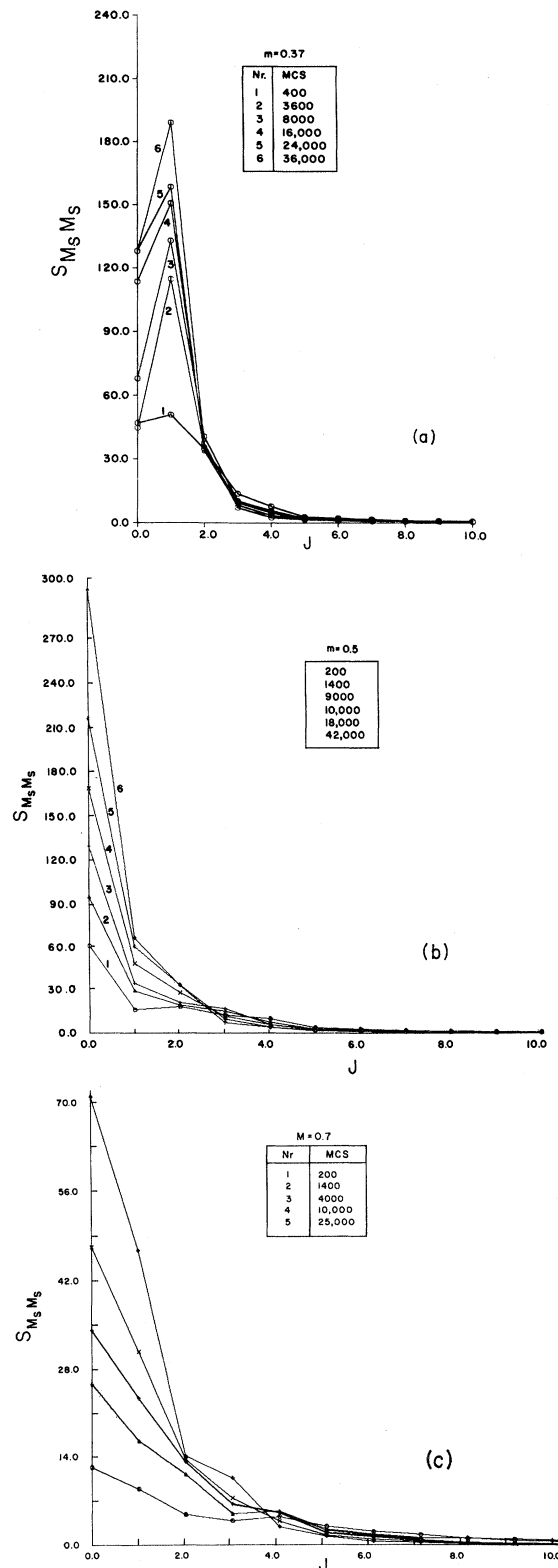


FIG. 5. The sublattice structure factors $S_{M_s M_s}$ vs j for points (a) P_1 , (b) P_2 , and (c) P_3 . Time in Monte Carlo steps for different curves is given in the inset.

able the behavior of $S_{MM}(k,t)$ is quite similar to the structure function for the local concentration of one species of atom in a binary alloy. As can be seen in Figs. 6(a)–6(c) the phase separation process (spinodal decomposition) reflects itself in a peak in $S_{MM}(k,t)$ at a nonzero value of k , $k_m(t)$, which gradually decreases with increasing time. It is difficult to make an accurate estimate of the value of $k_m(t)$ (or of $S(k_m(t),t)$) because we are monitoring only discrete values of k . We will find it more useful to examine the moments of S_{MM} , as discussed in the next section. One interesting qualitative point, however, which does emerge from our results is the asymmetry in the structure function $S_{MM}(k,t)$ as a function of the magnetization. In the case of a binary alloy whose phase diagram is symmetric about the critical point value of the concentration (which is the analog of M in our phase diagram), the structure function is of course itself symmetric. The system is most unstable at a quench at the critical value of the concentration and less so as one quenches on either side of this critical value. In the tricritical case no such symmetry with respect to M exists and the system is neither maximally unstable at M_t , nor symmetric with respect to this tricritical value. This can be seen even within the errors encountered in our MC work (Table I) by an examination of $S_{MM}(k,t)$ at any given time for the three quenches P_1 , P_2 , and P_3 . It seems quite clear that for a given t the largest value of $S_{MM}(k_m(t),t)$ occurs at $M=0.7$ and that the smallest value of $S_{MM}(k_m(t),t)$ occurs at $M=0.37$. That is, it would appear that in this region $S_{MM}(k_m,t)$ increases as M increases for fixed t . It is also obvious that this

TABLE I. The magnetic structure factor $S_{MM}(k,t)$ at selected values of time for points P_1 , P_2 , and P_3 , for model I.

MCS	$S_{MM}(k_m(t),t)$		
	P_1	P_2	P_3
400	1.0	2.0	2.0
2800	2.1	4.1	4.3
12 000	4.6	6.9	8.0
16 000	5.1	6.7	9.9
20 000	6.1	9.0	11.5
26 000	7.9	11.0	14.0
36 000	10.2	13.7	...
42 000	...	13.9	...

behavior cannot continue indefinitely as one moves towards the right-hand branch of the coexistence curve. It is therefore of some interest to determine where this increase in $S_{MM}(k_m,t)$ ceases. We have thus performed a preliminary study of this question by examining the behavior at several other values of M . We have found that as one increases M the peak drops rather dramatically at fixed t (even for rather early times) in a very narrow region around $M \approx 0.88$. A more detailed analysis of this transition region and the cluster dynamics will be presented elsewhere.

At least a qualitative understanding of why this asymmetry and sharp transition occurs can be gained from a mean-field, linear stability analysis. In this

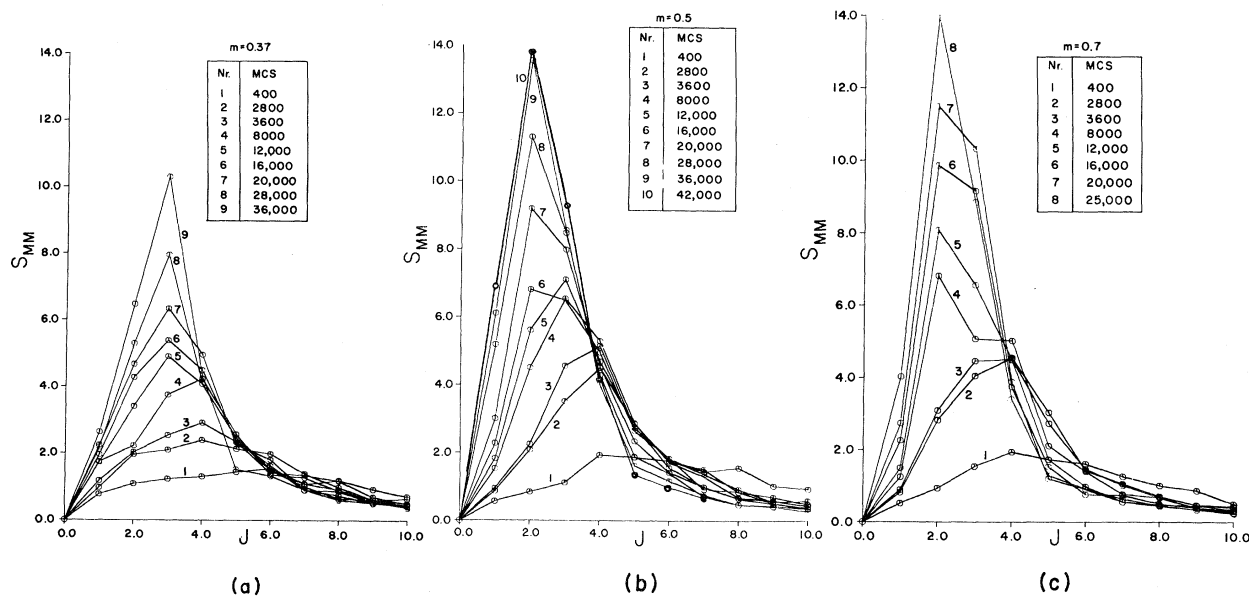


FIG. 6. The magnetic structure factors S_{MM} vs j for points (a) P_1 , (b) P_2 , and (c) P_3 . Time in Monte Carlo steps for different curves is given in the inset.

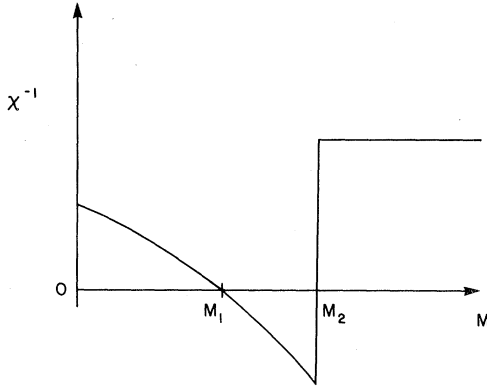


FIG. 7. The mean-field susceptibility χ as a function of magnetization M at a fixed temperature.

case the Fourier component M_k of the local magnetization density is assumed to be given by a linearized equation of motion such that the resultant structure factor is

$$S_{MM}(k, t) = S_{MM}(k) \exp[-\Gamma k^2(k^2 + \chi^{-1})t], \quad (2.15)$$

where Γ is a kinetic coefficient. The mean-field approximation for the effective susceptibility which arises from an adiabatic elimination of the nonconserved order parameter in this Cahn-like theory is shown in Fig. 7. What is notable, as mentioned in the Introduction, is that χ^{-1} becomes more negative as M increases from one spinodal point, M_1 , to the other, M_2 , rather than being symmetric about a critical value, as for simple binary alloys. Thus the instability in S_{MM} increases (for $k < |\chi^{-1}|$) as one increases M until $M > M_2$, where in the classical theory one would be in the metastable region. This is qualitatively consistent with what we see. This linear theory is, however, incorrect in many details, including its prediction that $S_{MM}(k, t)$ should exhibit exponential growth as a function of time. A more detailed Langer-Bar-on, Miller-like theory³⁴ has been carried out by Dee *et al.*³⁵ which does not exhibit exponential growth but does predict similar asymmetric behavior. However, as noted in the Introduction it is at the moment not possible for us to give a more precise explanation of this transition beyond that mentioned above. Further theoretical work on this point is clearly needed.

III. SCALING

We now turn to the question of whether or not the structure functions for the tricritical model exhibit a scaling behavior with respect to certain time dependent wave numbers which one might define for the system. It is first worth noting, as has been exten-

sively discussed in the MC studies of binary alloys, that it will be difficult to make detailed comparisons between the $S(k, t)$ obtained in our work and the more smooth structure functions which one might expect to see in experimental or theoretical studies of such a system. This problem is due to the discrete nature of our computer results, i.e., to the discrete set of k values studied. In addition, of course, there is considerable fluctuation in our data, particularly for the structure factor with nonconserved order parameter. Both of these effects are due to the small size of our system ($N = 3600$ spins) as compared to the macroscopic systems studied in theory or experiment, in which N is essentially infinite. In spite of these problems one might hope that certain features of our results exhibit a certain smoothness more typical of real systems, as well as provide some qualitatively interesting predictions to be tested by theory and/or experiment. With this in mind we have calculated various moments of the two structure functions, defined as

$$k_n(t) = \frac{\sum^{k_c} k^n S(k, t)}{\sum^{k_c} S(k, t)} \quad (3.1)$$

for each of the two functions. In the case of $S_{MM}(k, t)$ both the odd and even moments are of interest. On the other hand $S_{M_s M_s}(k, t)$ is an even function of k , so that it is only necessary to calculate the even moments. However, we have also monitored the magnitude of its first moment, i.e.,

$$|k_1| = \frac{\sum^{k_c} |k| S_{M_s M_s}(k, t)}{\sum^{k_c} S_{M_s M_s}(k, t)}. \quad (3.2)$$

It is necessary to note three points concerning the above definitions. First of all, as for the case of the binary alloy our results for the moments are sensitive to the choice of the upper cutoff k_c , which in the ideal case of extremely accurate data for large k should be chosen to be π , the upper Brillouin zone value consistent with periodic boundary conditions. However, our structure functions are very small for large k , as can be seen from Figs. 5 and 6, with fluctuations being comparable to the actual values. We have therefore chosen k_c as $(2\pi)10/\sqrt{N}$. We have examined the dependence of our results on smaller values of k_c and have concluded that the choice used is quite reasonable. The second point concerns a far more serious problem for the moments of $S_{M_s M_s}(k, t)$. Namely, our estimates for its moments and their time dependence are extremely sensitive to the minimum value of k entering in (3.1), as we noted in the Introduction. This sensitivity depends on the fact that the important contributions to the denominator $S_{M_s M_s}(k, t)$ in (3.1) come from small k . Since the sublattice structure factor at the origin, $S_{M_s M_s}(k=0, t) = NM_s^2(t)$, strongly reflects

the “metastability” which we encounter, our results for the moments of $S_{M_s M_s}(k, t)$ are quite sensitive to its value at $k = 0$. On the other hand, we have used periodic boundary conditions for convenience, since in the bulk limit our results should not depend on the boundary conditions. Unfortunately in this case we seem to encounter rather strong “finite-size” effects related to the nature of the boundary conditions. Had we used “free edge” boundary conditions, we would not have included $k = 0$ contribution since the smallest allowed k would then be $k_{\min} = 2\pi/L$, where L is the linear dimension of the system. Motivated by these considerations we have therefore analyzed our moments of $S_{M_s M_s}$ with and without the $k = 0$ data and have found a much more consistent scaling picture for the case without the $k = 0$ data. It should be stressed, however, that due to the above difficulty our estimates for the time dependence of the moments of $S_{M_s M_s}(k, t)$ are not very convincing.

The third point is that in contrast to the recent MC studies of the binary alloy we have chosen not to subtract off the equilibrium values of the structure functions entering in Eqs. (3.1) and (3.2), since as we will see our results scale quite reasonably using the moments as defined in (3.1). As can be seen in Fig. 8 the moments for both $S_{M_s M_s}$ and S_{MM} behave quite smoothly as a function of time.

One can also attempt to approximate the time dependence of these moments by simple power-law behavior in different time domains, as has been done in previous MC studies of binary alloys² and order-disorder transitions.⁹ For example, one can try approximations of the form

$$|k_1(t)| \sim t^{-a} \quad (3.3)$$

and

$$\sqrt{k_2(t)} \sim t^{-a'} \quad (3.4)$$

for the moments of $S_{M_s M_s}(k, t)$ subject to the reservations about $k = 0$ noted above. In addition, one can do the same for $S_{MM}(k, t)$, i.e.,

$$k_1(t) \sim t^{-b}, \quad (3.5a)$$

$$\sqrt{k_2(t)} \sim t^{-b'}. \quad (3.5b)$$

Typically what one finds in studies of the binary alloy is that the value of such exponents depends on the time intervals studied. It is therefore not completely clear that such approximations are of significance except possibly in certain time domains where such approximations are of significance except possibly in certain time domains where such asymptotic behavior might be expected (as, for example, $k_1 \sim t^{-1/3}$ in the Lifshitz Slyozov late stage region for an alloy). With this qualification in mind we present in Table II the

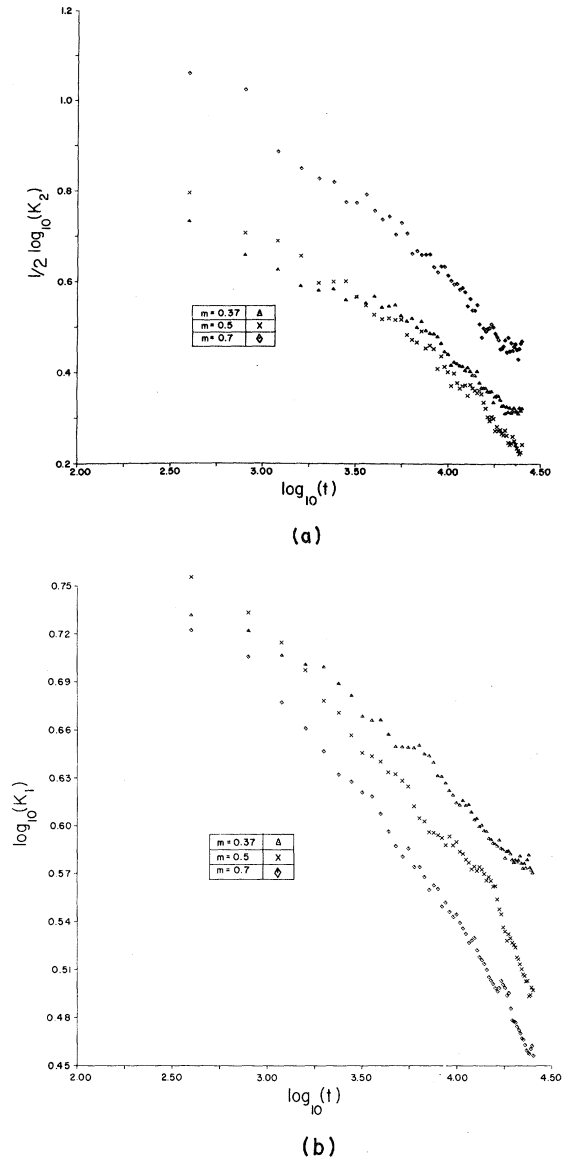


FIG. 8. (a) $\text{Log}_{10}k_2$ vs $\text{log}_{10}t$ for points P_1 , P_2 , and P_3 . (b) $\text{Log}_{10}k_1$ vs $\text{log}_{10}t$ for points P_1 , P_2 , and P_3 .

results of such power-law fits both for the entire time domain studied (so called “effective exponents” which might have no significance) as well as for certain select time intervals where a simple power-law approximation seems more reasonable. We observe two facts from this table. First, for the late time region of our study we see that the exponent $b \approx 0.14$ for P_1 , increases to $b \approx 0.25$ for P_2 and then decreases to $b \approx 0.21$ for P_3 . A rather similar behavior has been observed by Dee *et al.*³⁵ in their study of a three-dimensional tricritical system, although the values of b are different from our two-dimensional

TABLE II. The "effective", early and late time exponents of the first and the second moments of the sublattice and magnetic structure factors for P_1 , P_2 , and P_3 .

M	Time intervals in MCS		a	a'	b	b'
0.37	400	36 000	0.10	0.11	0.12	0.11
	400	6000	0.11	0.10	0.08	0.07
	6000	36 000	0.10	0.12	0.14	0.13
0.5	200	42 000	0.12	0.11	0.17	0.15
	200	10 000	0.10	0.09	0.13	0.11
	10 000	42 000	0.12	0.12	0.25	0.21
0.7	200	25 200	0.15	0.14	0.17	0.16
	200	10 000	0.14	0.13	0.14	0.13
	10 000	25 200	0.15	0.16	0.21	0.20

results. Second, the scaling concept suggests that $a = a'$ and $b = b'$ which, as can be seen from Table II, is consistent with our results. The overall picture, however, is relatively consistent, since as shown both in Tables II and III the data seem compatible with the notion that is a single scaling length for each structure function. In Table III we show the ratios of the various relevant moments. These ratios should be independent of time in a scaling domain. As can be seen from Table III this seems to be reasonably well satisfied. A very weak dependence on time is, however, detectable in Table III, as has been seen in Ref. 7 and some recent work on binary fluids.³⁸ It should also be noted that the results presented for $S_{M_s M_s}(k, t)$ in Tables II and III *exclude* the data for

$k = 0$. If one includes the $k = 0$ data, then the picture for scaling for this correlation function seems much less convincing, since the ratio $k_1/\sqrt{k_2}$ then displays a much stronger dependence on time than shown in Table III. In addition, the exponents a and a' change considerably if one includes the $k = 0$ data, particularly for $M = 0.5$ and $M = 0.7$ where they are consistently larger (by as much as a factor of 2) than those shown in Table II. As well, the exponents a and a' differ considerably from each other (in contrast to the expected scaling result $a = a'$) if one includes the $k = 0$ data. It should also be stressed, however, that if one does not use predictions of scaling (such as $a = a'$ or the constancy of $k_1(t)/\sqrt{k_2(t)}$) as a test of the scaling behavior, but rather simply re-

TABLE III. The ratio of the second and the first moments for both the magnetic and sublattice structure factors at selected times.

M	MCS	10 000	12 000	14 000	16 000	18 000	20 000	24 000	28 000	32 000	36 000	42 000
0.37	$\left(\frac{\sqrt{k_2}}{k_1}\right)_M$	1.13	1.13	1.13	1.13	1.13	1.13	1.14	1.14	1.14	1.14	...
	$\left(\frac{\sqrt{k_2}}{ k_1 }\right)_{M_s}$	1.29	1.28	1.28	1.28	1.27	1.26	1.26	1.25	1.25	1.24	...
0.5	$\left(\frac{\sqrt{k_2}}{k_1}\right)_M$	1.13	1.13	1.13	1.14	1.15	1.15	1.16	1.16	1.17	1.17	1.17
	$\left(\frac{\sqrt{k_2}}{ k_1 }\right)_{M_s}$	1.25	1.25	1.25	1.26	1.25	1.25	1.26	1.25	1.25	1.24	1.25
0.7	$\left(\frac{\sqrt{k_2}}{k_1}\right)_M$	1.14	1.14	1.14	1.14	1.14	1.13	1.14
	$\left(\frac{\sqrt{k_2}}{ k_1 }\right)_{M_s}$	1.28	1.27	1.26	1.26	1.26	1.26	1.26

lies on a "visual" test $S_{M_3 M_3} = k_2^{-1}(t) F(k/\sqrt{k_2})$ there is little to discriminate between our "scaling results" for $S_{M_3 M_3}(k, t)$ for the two cases with $k = 0$ either included or excluded.

Finally, we turn to the question of the scaling functions. We first discuss the situation for $S_{M_3 M_3}(k, t)$. Here we have attempted to analyze our data in the form

$$S_{M_3 M_3}(k, t) = k_2^{-1}(t) G(y), \quad (3.6)$$

where $y = k/\sqrt{k_2(t)}$. We have excluded the early time data as well as the $k = 0$ points from the analysis. As can be seen from Figs. 9(a)–9(c) the data for all three quenches P_1 , P_2 , and P_3 , satisfy a scaling of this form, where the scaling function $G(y)$ seems to exhibit a weak dependence of M for large

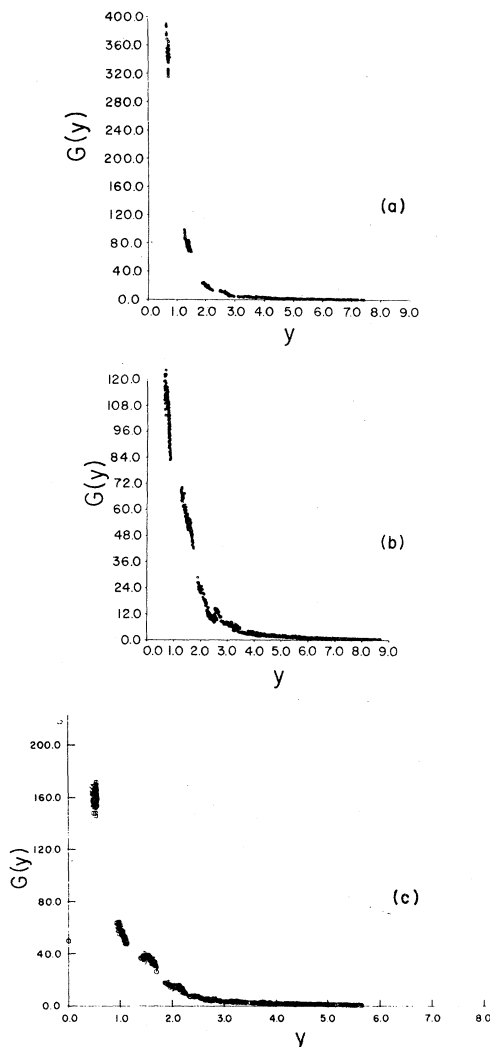


FIG. 9. The scaled sublattice structure factors $G(y)$ vs y for points (a) P_1 , (b) P_2 , and (c) P_3 .

values of y . It should further be noted that the small y region is strongly M dependent. In Fig. 9(c) there is some scatter in the data around $y = 1.75$ but otherwise the scaling of the data seems quite reasonable.

The other structure function, $S_{MM}(k, t)$, is of more interest in this regard since there is clearly much more "structure" in this function than for $S_{M_3 M_3}$.

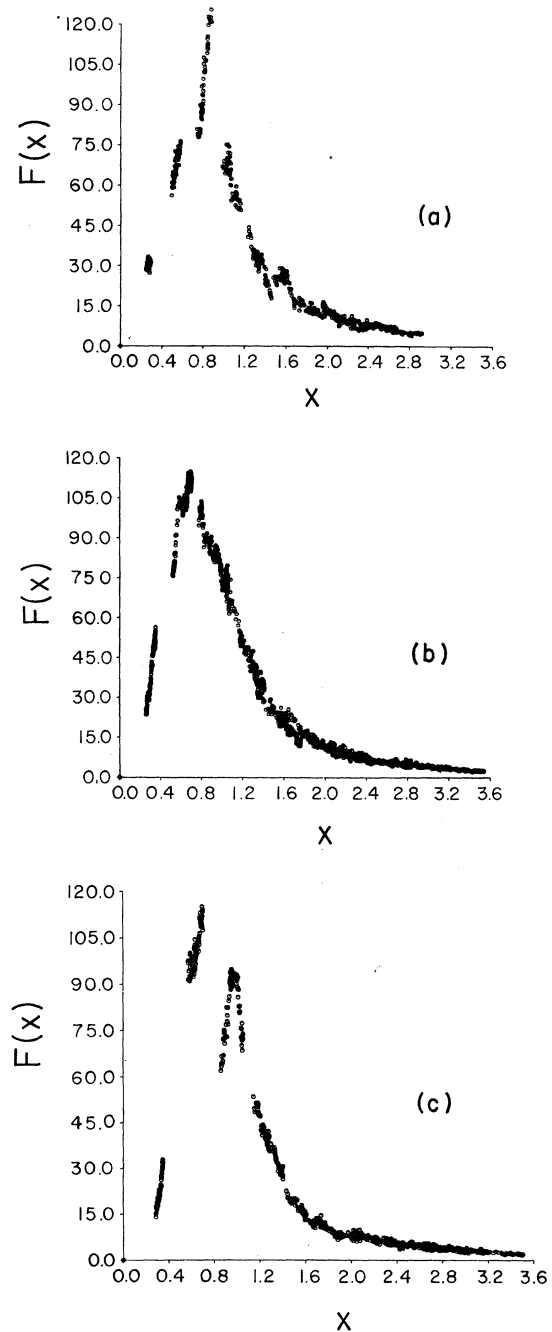


FIG. 10. The scaled magnetic structure factors $F(x)$ vs x for points (a) P_1 , (b) P_2 , and (c) P_3 .

TABLE IV. The ratio of the first moment of the magnetic structure factor with (a) the square root of the second moment of the sublattice structure factor and (b) the “first moment” of the sublattice structure factor, respectively, at the specified times for P_1 , P_2 , and P_3 .

M	MCS	10 000	12 000	14 000	16 000	18 000	20 000	24 000	28 000	32 000	36 000	42 000
0.37	$\frac{(k_1)_M}{(\sqrt{k_2})_{M_s}}$	2.06	2.08	2.04	2.06	2.07	2.10	2.10	2.08	2.02	2.04	...
	$\frac{(k_1)_M}{(k_1)_{M_s}}$	2.65	2.65	2.61	2.63	2.66	2.64	2.60	2.52	2.52
0.50	$\frac{(k_1)_M}{(\sqrt{k_2})_{M_s}}$	1.50	1.48	1.49	1.51	1.46	1.46	1.40	1.36	1.36	1.32	1.29
	$\frac{(k_1)_M}{(k_1)_{M_s}}$	1.87	1.85	1.86	1.90	1.83	1.83	1.77	1.69	1.70	1.64	1.61
0.70	$\frac{(k_1)_M}{(\sqrt{k_2})_{M_s}}$	1.39	1.32	1.32	1.30	1.30	1.30	1.26
	$\frac{(k_1)_M}{(k_1)_{M_s}}$	1.71	1.68	1.67	1.65	1.65	1.64	1.59

Here we have analyzed our data in the form

$$S_{MM}(k, t) = k_1^{-2}(t) F(x) \quad (3.7)$$

where $x = k/k_1(t)$. As can be seen from Figs. 10(a)–10(c) we again find reasonable evidence for scaling behavior, although the data are not completely consistent with a smooth scaling function $F(x)$. The best fit to a smooth function seems to occur at $P_2(M=0.5)$ as can be seen in Fig. 10(b). At both P_1 and P_3 , however, there is an apparent departure from a smooth scaling for values of x in the range 0.8 to 1 which we believe to be due to an “accidental” erratic behavior of our Monte Carlo results for $S_{MM}(k, t)$ at $j=3$.

One interesting question which cannot be completely settled by our present work is whether there are one or two characteristic lengths in this problem. We have chosen to scale our data for each structure function with its appropriate moment. However, it is natural to ask whether the ratio of these two inverse lengths might be time independent. In Table IV we show the ratio of $(k_1)_M/(\sqrt{k_2})_{M_s}$ where $(\sqrt{k_2})_{M_s}$ and $(k_1)_M$ refer to $S_{M_s M_s}$ and S_{MM} , respectively. As can be seen from the table, it would appear that these two inverse lengths are in fact different.

IV. MONTE CARLO RESULTS FOR MODEL II

As mentioned in the Introduction, an earlier Monte Carlo study²¹ of spinodal decomposition for the system described by the Hamiltonian in (2.1) was

carried out for a quench to P_2 . In this case, however, the transition probability given in (2.2) also included next-nearest neighbor exchanges. No distinction was made between the time to spin exchange nearest or next-nearest-neighbor pairs, with the transition probability being given by (2.2) for either type of exchange. In this section we report on some other properties of this model II (NN and NNN exchange) and compare these with the results given in II and III for model I. It should be noted that one qualitative distinction that is readily apparent between these two models is that the inclusion of next-nearest-neighbor spin exchange allows the system to evolve more rapidly in time than it would otherwise.

To begin with, we recall that in the original work the scaling function $S_{M_s M_s}(k, t)$ exhibited a scaling behavior of the form $t^{-0.7} F(kt^{0.35})$ in the range³⁹ 2100–4200 MCS quite similar to that shown in Fig. 9. This amounts to assuming a power-law approximation for $K(t)$ of $t^{-0.35}$ although in the original work no attempts were made to calculate moments to possibly justify this scaling. It should be noted that we were also able to find a somewhat less satisfactory scaling using an effective length $K(t) \sim t^{-x}$ with x anywhere in a wide range of values. The choice $x=0.35$ seemed to give the least deviations from a smooth scaling but as noted in Ref. 21 this was only an approximate estimate. In this section we present our results for the moments of $S_{M_s M_s}(k, t)$ and $S_{MM}(k, t)$ and reexamine the scaling of these functions. We begin by considering the moments of $S_{M_s M_s}(k, t)$ in which we exclude the $k=0$ data. In

TABLE V. The "effective" and late time exponents of the first and the second moments of the sublattice and magnetic structure factors at $M=0.5$ and $T=0.6T_c$.

M	Time interval in MCS	a	a'	b	b'
0.5	150–4200	0.15	0.14	0.19	0.17
	1500–4200	0.17	0.16	0.21	0.19

Table V we show the time dependence for $|k_1(t)|$ and $k_2(t)$ for this model. As can be seen from the table there is no simple power-law approximation which fits the data in the entire time domain considered. If one "forces" a fit to a single effective exponent one finds an exponent of $a=0.15$ for $|k_1|$ and $a'=0.14$ for $\sqrt{k_2}$. A more meaningful analysis would appear to be to consider a power-law approximation in just the late time region where there seems to be more convincing evidence for simple power-law behavior. As shown in Table V this yields exponents $a=0.17$ and $a'=0.16$. Since the latter numbers would seem to be more meaningful than exponents obtained from using the entire time region, it would seem that our results for $S_{M_s M_s}$ are in fact reasonably consistent. As can be seen from Table VI the ratio $\sqrt{k_2}/|k_1|$ is approximately time independent as it should be if scaling is valid. It should be noted, however, that the scaling for $S_{M_s M_s}(k, t)$ using k_2 implies and effective exponent ($\sqrt{k_2} \sim t^{-a}$) with the value considerably different from the value of 0.35 quoted in the first study. This would seem to be a reflection of the fact (noted in the original paper) that a rather wide range of values for a will in fact "scale" the data reasonably well. It seems difficult to accurately determine a "best" exponent by this type of criterion alone, due to the inaccuracy of the Monte Carlo data. A much more stringent test of scaling is to consider whether or not ratios of moments of $S_{M_s M_s}(k, t)$ are

time independent. Finally we note that if we include the $k=0$ data, the estimates for the exponents a and a' change considerably by as much as a factor of 2. The result is that the exponents for models I and II would then appear to be significantly different, which is not the case when we exclude the $k=0$. In addition, the ratio of $|k_1|/\sqrt{k_2}$ is no longer time independent. Thus the overall picture seems much more consistent if one excludes the $k=0$, although this is of course not a compelling argument. In Table VII we display the ratios of $(k_1)_M/(\sqrt{k_2})_{M_s}$ and $(k_1)_M/|k_1|_{M_s}$, which slowly change with time. This suggests that these two inverse lengths are in fact different.

The situation for $S_{MM}(k, t)$ is also quite reasonable. As can be seen from Table V, the exponents b and b' which characterize k_1 and $\sqrt{k_2}$ for this function are approximately equal. In addition S_{MM} exhibits a scaling similar to model I (Fig. 10). Also, the "late time" behavior for this model (i.e., 1500–4200 MCS) is almost the same as that for model I, particularly at $M=0.5$ and $M=0.7$, in the regions 10 000–42 000 and 10 000–25 000, respectively. Indeed, given the large fluctuations involved in the MC data in both cases, the overall behavior of $S_{M_s M_s}(k, t)$ and $S_{MM}(k, t)$ for both models is very similar. We see no strong evidence at the moment to suggest that these two models have significantly different dynamical properties.

TABLE VI. The ratio of the square root of the second moment and the first moment for both the magnetic and sublattice structure factors at selected times.

MCS	300	900	1500	2100	2700	3300	3900	4200	
$M=0.5$	$\left(\frac{\sqrt{k_2}}{ k_1 }\right)_M$	1.12	1.13	1.16	1.16	1.17	1.17	1.18	1.17
	$\left(\frac{\sqrt{k_2}}{ k_1 }\right)_{M_s}$	1.27	1.28	1.29	1.28	1.30	1.31	1.30	1.30

TABLE VII. The ratio of the first moment of the magnetic structure factor with (a) the square root of the second and (b) "first moment" of the sublattice structure factor, respectively, at $M=0.5$ and $T=0.6T_c$.

MCS	300	900	1500	2100	2700	3200	3900	4200
$\frac{(k_1)_m}{(\sqrt{k_2})_{M_s}}$	1.62	1.60	1.50	1.45	1.44	1.43	1.42	1.43
$M=0.5$								
$\frac{(k_1)_M}{(k_1)_{M_s}}$	2.03	2.05	1.94	1.85	1.87	1.87	1.85	1.85

V. CONCLUSION

Our investigation of tricritical spinodal decomposition in a two-dimensional model of an Ising metamagnet or, equivalently, a simple model of chemisorption, has revealed two major features. The first is that the structure functions S_{MM} and $S_{M_s M_s}$ exhibit, to a good first approximation, a simple scaling behavior. The second is the unusual asymmetry and corresponding sharp transition in the peak height behavior of S_{MM} which has not been seen in previous studies of binary alloys and binary fluids. This second feature would seem to distinguish "tricritical" spinodal decomposition from "critical" spinodal decomposition. Although one can imagine alloys with asymmetric coexistence curves, it seems less likely that such systems would have such strongly asymmetric susceptibilities (vis-a-vis the discontinuous mean-field effective susceptibility) as in our case. As a consequence, the sharp transition which we have seen would seem less likely to occur in a system quenched below its critical point. It would be interesting to have experimental tests of such asym-

metric behavior, which is certainly not limited to two-dimensional systems. One possible candidate for study is Fe-Al, alloy which is thought to have a tricritical point.⁴⁰ Another possible system is ^3He - ^4He , although this system has hydrodynamic modes not included in our model. Nevertheless ^3He - ^4He does have the same mean-field effective susceptibility shown in Fig. 7, so that it is possible some manifestation of an asymmetry and sharp transition could be seen in light scattering studies. In addition, it would be worth having experimental studies of scaling in tricritical systems. Very recent studies⁴¹ of ^3He - ^4He in fact seem to show scaling quite similar to what we have reported here. Finally we note that there is clearly a need for a better theoretical understanding of the nonlinear dynamics of tricritical systems.

ACKNOWLEDGMENTS

This work was supported in part by a grant from the NSF Grant No. DMR-8013700. It was also supported by a grant to S.K. from the Research Corpora-

¹G. Laslaz and P. Guyot, *Acta Metall.* **25**, 277 (1977); G. Laslaz, P. Guyot, and G. Kostorz (unpublished).

²S. P. Singhal, H. Herman, and G. Kostorz (unpublished).

³P. A. Flinn, *J. Stat. Phys.* **10**, 89 (1974).

⁴A. B. Bortz, M. H. Kalos, and J. L. Lebowitz, *Phys. Rev. B* **10**, 535 (1974).

⁵J. Marro, A. B. Bortz, M. H. Kalos, and J. L. Lebowitz, *Phys. Rev. B* **12**, 2000 (1975).

⁶K. Binder, M. H. Kalos, L. J. Lebowitz, and J. Marro, *Adv. Colloid Interface Sci.* **10**, 173 (1979).

⁷J. L. Lebowitz, J. Marro, and M. H. Kalos (unpublished).

⁸G. F. Nielson, *Phys. Chem. Glasses* **10**, 54 (1969).

⁹P. T. van Emmerik, C. A. Smolders, and W. Geymayer, *Eur. Poly. J.* **9**, 309 (1973).

¹⁰L. P. McMaster, *Adv. Chem. Ser.* **142**, 43 (1975).

¹¹T. Nishi, T. T. Wang, and T. K. Kwei, *Macromolecules* **8**, 227 (1975).

¹²P. G. deGennes, *J. Chem. Phys.* **72**, 4756 (1980).

¹³W. Goldburg, A. J. Schwartz, and M. W. Kim, *Prog. Theor. Phys. Suppl.* **64**, 477 (1978).

¹⁴Y. C. Chou and W. Goldburg, *Phys. Rev. A* **20**, 2105 (1979).

¹⁵Y. C. Chou and W. Goldburg, *Phys. Rev. A* **23**, 858 (1981).

¹⁶N. C. Wong and C. M. Knobler, *J. Chem. Phys.* **69**, 725 (1978); *Phys. Rev. Lett.* **43**, 1733 (1979).

¹⁷E. Siggia, *Phys. Rev. A* **20**, 595 (1979).

¹⁸P. C. Hohenberg and D. R. Nelson, *Phys. Rev. B* **20**, 2665 (1979).

¹⁹J. K. Hoffer, L. J. Campbell, and R. J. Bartlett, *Phys. Rev.*

- Lett. 45, 912 (1980).
- ²⁰T. Benda, P. Alpern, and P. Leiderer (unpublished).
- ²¹P. S. Sahni and J. D. Gunton, Phys. Rev. Lett. 45, 369 (1980).
- ²²J. Marro, J. L. Lebowitz, and M. H. Kalos, Phys. Rev. Lett. 43, 282 (1979).
- ²³M. K. Phani, J. L. Lebowitz, M. H. Kalos, and O. Penrose, Phys. Rev. Lett. 45, 366 (1980).
- ²⁴P. Sahni, G. Dee, J. D. Gunton, M. Phani, J. L. Lebowitz, and M. H. Kalos, Phys. Rev. B (in press).
- ²⁵H. Hennion, D. Ronzand, and P. Guyot (unpublished).
- ²⁶H. Furukawa, Phys. Rev. Lett. 43, 136 (1979).
- ²⁷K. Kawasaki, C. Yalabik, and J. D. Gunton, Phys. Rev. B 17, 455 (1978).
- ²⁸G. Doyen, G. Ertl, and M. Plancher, J. Chem. Phys. 62, 2957 (1975).
- ²⁹S. Kono, S. M. Goldbreg, N. F. T. Hall, and C. S. Fadley, Phys. Rev. B 22, 6085 (1980).
- ³⁰K. H. Lau and S. C. Ying, Phys. Rev. Lett. 44, 1222 (1980).
- ³¹P. Sahni and J. D. Gunton (unpublished).
- ³²D. P. Landau and R. H. Swendsen (unpublished).
- ³³D. P. Landau, Phys. Rev. Lett. 28, 449 (1972).
- ³⁴J. S. Langer, M. Bar-on, and H. D. Miller, Phys. Rev. A 11, 1417 (1975).
- ³⁵G. Dee, J. D. Gunton, and K. Kawasaki, Prog. Theor. Phys. (in press).
- ³⁶I. M. Lifshitz and V. V. Slyozov, J. Phys. Chem. Solids 19, 35 (1961).
- ³⁷M. San Miguel, J. D. Gunton, G. Dee, and P. Sahni, Phys. Rev. B 23, 2334 (1981).
- ³⁸C. Knobler (private communication).
- ³⁹In Ref. 21 we used a unit of time in which attempted exchanges between like spins were not included. To convert the time unit used in that paper to the standard Monte Carlo step used in this work one must multiply it by a factor of 3/2. In addition average value $\langle \sigma \rangle$ was inadvertently omitted in the definition of the magnetic structure factor.
- ⁴⁰S. M. Allan and J. W. Cahn, Acta Metall. 24, 425 (1976).
- ⁴¹D. N. Sinha and J. K. Hoffer (unpublished).